

# Component Segmentation of Engineering Drawings Using Graph Convolutional Networks

Wentai Zhang, Joe Joseph, Yue Yin, Liuyue Xie, Tomotake Furuhata, Soji Yamakawa, Kenji Shimada, Levent Burak Kara\*

*Department of Mechanical Engineering, Carnegie Mellon University, Pittsburgh, PA, 15213, USA*

---

## Abstract

We present a data-driven framework to automate the vectorization and machine interpretation of 2D engineering part drawings. In industrial settings, most manufacturing engineers still rely on manual reads to identify the topological and manufacturing requirements from drawings submitted by designers. The interpretation process is laborious and time-consuming, which severely inhibits the efficiency of part quotation and manufacturing tasks. While recent advances in image-based computer vision methods have demonstrated great potential in interpreting natural images through semantic segmentation approaches, the application of such methods in parsing engineering technical drawings into semantically accurate components remains a significant challenge. The severe pixel sparsity in engineering drawings also restricts the effective featurization of image-based data-driven methods. To overcome these challenges, we propose a deep learning based framework that predicts the semantic type of each vectorized component. Taking a raster image as input, we vectorize all components through thinning, stroke tracing, and cubic bezier fitting. Then a graph of such components is generated based on the connectivity between the components. Finally, a graph convolutional neural network is trained on this graph data to identify the semantic type of each component. We test our framework in the context of semantic segmentation of text, dimension and, contour components in engineering drawings. Results show that our method yields the best performance compared to recent image, and graph-based segmentation methods.

*Keywords:* engineering drawings, graph neural networks, component segmentation, deep learning, computer vision

---

## 1. Introduction

Engineering technical drawings serve as a universal medium for information exchange between designers and manufacturers. Such drawings encode the topological information, dimensions, and manufacturing requirements of a product in a unified and standard form, which can then be utilized in various engineering applications including content-based part indexing [1, 2], cost estimation [3] and process planning [4]. While the underlying designs are commonly created in a vector format through digital design tools, they are often discriminated to manufactures as raster images due to the ease of information exchange and quality assurance. According to a survey in Japan's manufacturing industry [5], 84% of the customers use 2D raster-based drawings such as PDF, paper, or fax format when placing an

order for manufacturing, which results in a major impediment in the automation of the aforementioned applications due to the need of human involvement in interpreting these drawings.

For a modern online platform of part manufacturing, clients often upload their designs in raster image format for better quality assurance and IP protection since the information in image drawings are ineditible. Unlike a vector format, which enables a trivial digital access to all stored information through a script file, raster drawings usually require manual inspection by technicians to extract the information required for quotation and manufacturing. The inspection process includes the identification of the part shape, dimensions, and manufacturing requirements.

Here, we focus on the problem of semantic segmentation of the components in raster drawings. Common engineering components consist of straight lines, arcs, and circles. Our goal is to develop an automated data-driven

---

\*Address all correspondences to  
Email address: lkara@cmu.edu (Levent Burak Kara)

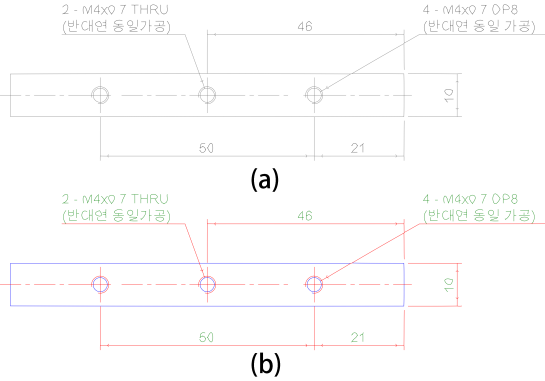


Figure 1: (a) Typical engineering drawing. (b) Semantically labeled results. Blue: Contours, Green: Texts, Red: Dimension sets.

framework that learns to distinguish between contour shapes, dimension sets, and text at the component level. Our approach improves the efficiency of technical drawing interpretation, relieving the burden of human operators by reducing the repetitive and tedious task of labeling drawings.

While recent vision-based methods have shown to be effective in image interpretation tasks such as object detection [6, 7, 8], semantic segmentation [9, 10, 11], and visual question answering [12, 13, 14], it is challenging to apply these methods to the segmentation of components in engineering drawings since the type of a component is also dependent on the contextual information. The same component can have different semantic meanings hence categories in different contexts. Engineering drawings typically involve lines or curves only sparsely filling the image frame, and without color or textual feature, making traditional image-based segmentation approaches ineffective at engineering drawing interpretation.

To address this issue, we present a new approach to engineering drawing segmentation that maps the components in the drawing to a graph structure embedded with contextual information (Fig. 2). The components are obtained through drawing preprocessing and a vectorization process, which then form the graph nodes. The relationships between the components are encoded in the edges in the graph. A set of features are computed as nodal attributes to embed the shape, size, curvature, and neighboring information. With this, the task of component segmentation of a raster drawing image is formatted as a node labeled problem.

Graph Convolutional Networks (GCNs) have shown great promise in node classification in various graph-structured data including academic networks [15], so-

cial networks [1], citation networks [16] and medical data [17, 18]. Like CNNs, GCNs aggregate information from a node and its neighboring nodes using a trainable unstructured feature map, which makes it applicable to graph data of any shape. In this work, we build our data-driven model based on GraphSAGE [19], a recent GCN model that aggregates the nodal information from the neighborhood structure, to predict the component type of each vectorized entity in raster drawings. The effectiveness of our graph representation is validated by the comparison between our proposed GCN methods and three vision-based or graph-based model for image segmentation. The depth of our proposed model is optimized through a parametric study of the number of convolutional layers in the model. Results indicate superior performance in both 2-class classification and 3-class classification tasks compared to our baseline models.

Our main contributions include:

- A vectorization method for raster drawings by skeletonizing, tracing, splitting, and cubic bezier curve fitting.
- A graph representation for the extracted components in engineering drawings embedded with domain-specific nodal attributes and contextual information.
- A data-driven framework that takes the vectorized component graphs as input and identifies the nodal component type for semantic segmentation.

## 2. Related Works

In this section, we review some prior works for the analysis of engineering drawings. In addition, as inspiration to our proposed framework, we also introduce recent advances in graph-based methods for image analysis and general data-driven methods for graph node classification.

### 2.1. Content-based Methods for Engineering Drawing

In the analysis of engineering drawings, content-based methods are broadly used for drawing match or retrieval. The key is to comprehend the basic elements in the drawings and define a measure of similarity. To detect the basic elements, Hough line transform [20], pixel blocks [21], patch groups [22] are utilized as representations for extensive matching or retrieval tasks. When an exemplar drawing is given, the matching process seeks the closest drawing in an existing pool under a similarity measure. Prior works propose distances between graph of decomposed topology [23], distances

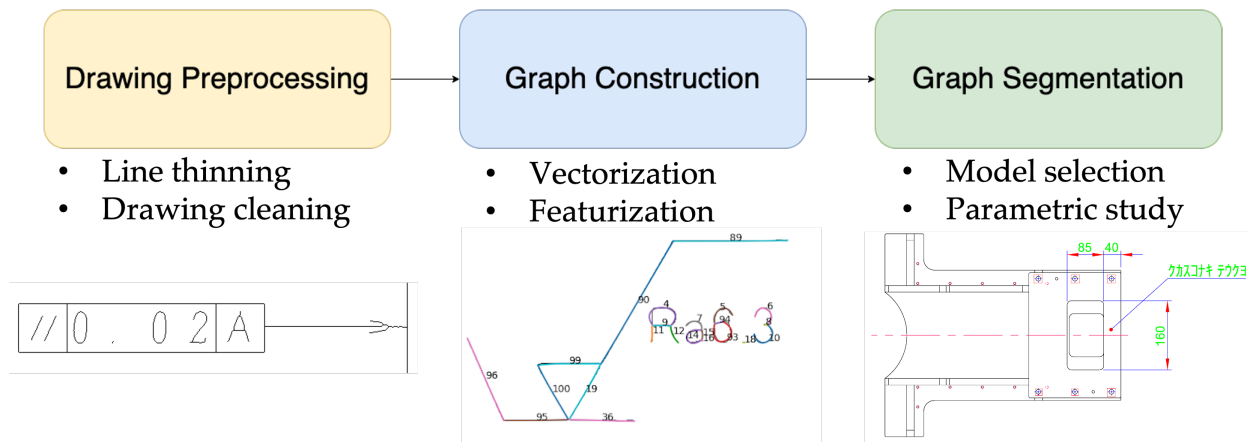


Figure 2: Our proposed workflow.

between feature vectors [20], weighted cosine similarity [24], and Bhattacharya correlation between histograms [25] to identify the most relevant drawing.

All works above are applied to drawings with only contour shapes, which restricts the extensive usage in our problem where the dimensions and texts are also included. But the idea of constructing a graph of basic elements enables an more efficient representation for raster drawings compared to the original image format.

## 2.2. Data-driven Methods for Graph Node Classification

When the graph of components is introduced, the problem of component segmentation is converted to the classification task of the graph nodes. Node classification is a critical problem in many supervised or semi-supervised learning scenarios [26]. Various methods have been proposed for node classification including iterative classification [16], label propagation [27], and SVM on nodal embeddings [28]. However, recent work has shown the promise of a better classification if the nodal embedding is jointly learned with the training of the data-driven classifier [29], which drives the development of end-to-end graph neural networks.

Since the first deep learning based framework, Deepwalk [30], is introduced to solve the nodal classification problem, graph neural networks have demonstrated their superior capability in efficient feature extraction on unstructured graph data. Recently, Graph Convolutional Networks (GCNs) [31] yield better performance due to the unique nodal information aggregation mechanism. Other variant of GCN extensively introduce various of ways for the aggregation including neighborhood aggregation [19] and attention mechanism [32], which

inspires us in building our proposed data-driven model for component segmentation.

## 2.3. Graph-based Methods for Image Analysis

For a more efficient and structured feature representation, graph models have been frequently introduced to multiple major tasks in image analysis. Monti et al. [33] propose the first GNN based method in image classification. More recent works focus on achieving the image segmentation using the graph of pixels [34] or graph of superpixels [35]. These oversegmented, simplified, images can be applied in many classic tasks in computer vision, including depth estimation, segmentation, and object localization [36].

The biggest advantage of introducing the graph representation in image analysis is that the problem can be decomposed into a higher level image processing with a more coarse unstructured data format. Unlike the image space where each pixel are treated as a independent element, the connection between the graph nodes enforces the possible dependencies due to the continuity of images. In engineering drawings, the type of a component is heavily dependent on the contextual information and the neighboring components. As such, we propose to vectorize the drawing as lower level component representation and construct graph of such vectors as the basic element for drawing analysis, embedding the contextual information in the edges of our component graph.

## 3. Technical Approach

In this work, we present a pipeline to preprocess engineering drawings, construct a labeled drawing dataset

and train a graph-based neural network model for component segmentation. This pipeline starts with a method that converts the raster drawing images into vectorized curves. Subsequently, a self-defined component graph is constructed based on the connections and distances among the obtained components. For each node (component) in the graph, we also present a novel featurization method to generate a series of feature parameters based on sampled points. Finally, this feature-embedded graph is utilized as input to a graph convolutional neural network that is able to predict the component type of each node (vector) in the drawing. Our inference pipeline is summarized in Algorithm. 1

---

**Algorithm 1:** Engineering Drawing Graph Network (EDGNet)

---

- Input :** A raster engineering drawing  $D_r$   
**Output:** A graph of vectorized components with semantic labeling  $G(N, E), Y$
- 1  $D_s \leftarrow \text{skeletonize}(D_r) + \text{smoothing};$
  - 2 Split  $D_s$  to strokes  $\{S_i\}_{n_N}$  from junction points;
  - 3 Fit cubic bezier curves  $\{B_i\}_{n_N}$  to each stroke  $S_i$ ;
  - 4 Init  $i = 1$ ;
  - 5 **while**  $i \leq n_N$  **do**
  - 6     Sample  $n$  equally spaced points  $P_i$  on  $B_i$ ;
  - 7     Calculate nodal features  $N \in \mathbb{R}^{n_N \times (4n-1)}$ ;
  - 8      $i = i + 1$ ;
  - 9 **end**
  - 10 Assemble a component graph  $G(N, E)$ ,  $E$  are the edges (connections) between the nodes;
  - 11 Get predicted semantic labels from a graph convolution network  $Y \in \mathbb{R}_N^n \leftarrow F_\theta(G(N, E))$
- 

### 3.1. Drawing Vectorization

As mentioned in Sec. 1, vision-based methods are not effective for feature extraction from raster engineering drawings since the information exists sparsely as discrete black pixels. Convolutional neural networks have severe limitations in embedding distant contextual information on very large images due to their ordered grid structure [37] and require endless increasing of depth. However, engineering drawings in their original vectorized form are capable to encode long-scale connectivity through an arbitrary graph structure. The basic elements of this graph structure consist of lines, curves, and texts of nodes and connectivity between them. As such, we propose a novel method to vectorize the raster drawings before analysis. The method consists of three broad steps: skeletonization, trajectory tracing, and curve fitting.

A CAD drawing is a collection of parametrically stored entities consisting of headers, blocks, tables, entities, and objects that can be easily rendered into a raster drawing through lines, curves, and text. However, it is challenging to identify these parameters from raster drawings due to the width of each entity and binary colors in the rendering process. As such, it is necessary to morphologically thin the drawing to identify the central trace of these strokes in raster drawings and extract the skeleton of each line for better fitting. In our implementation, three line thinning algorithms [38, 39, 40] were tested for extracting the skeleton out of the original drawing (Fig. 3). From the tests, it was concluded that the Medial Axis Transform method tends to generate more small branches where the line width is relatively large. The method from Lee’s cannot retain a complete structure for small components like the arrowheads. Zhang’s method does not produce clean junction points. Datta et. al. method was selected to have the most desirable thinned morphology for further processing and generating the parametric curves.

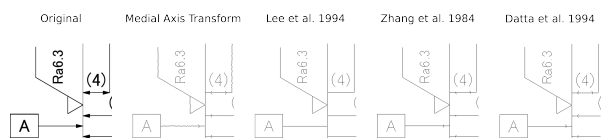


Figure 3: Comparison of four thinning methods in skeletonizing engineering drawings.

1. Thinning or skeletonization of the image to form traces with a single pixel width.
2. Smoothing the pixels to obtain a set of traces.
3. Splitting the traces to account for corners within the trace.
4. Removing small traces, and merging junction points
5. Fitting cubic bezier curves

Through the skeletonization process, strokes of lines and curves in the raster drawing are thinned to single pixel-wide trajectories. This allows us to trace the trajectories through neighboring pixels and convert the entire drawing into a unified set of parametric curves for better segmentation. In Fig. 4, we summarize three types of points existing in the obtained skeleton. The point type is defined based on the number of black pixels it connects to, which is efficiently calculated by a filter scanning over all the black pixels (Fig. 4(a)).

We define a trace as an ordered list of connected pixels starting from either a junction point or endpoint and

ending at either. To obtain this set of traces, we start at a randomly selected black pixel (Fig. 4(b)) and iteratively visit its neighboring points until a termination point (a junction or endpoint) has been reached. We then reverse the trace to reach the other termination point. This trajectory is recorded forming a completed trace used for parametric curve fitting. We continue this process until all black pixels have been visited and an entire set of traces have been created.

Now, with the set of pixel traces from the image, we split the traces if an edge is detected within the trace. To break the trace, we evaluated the cosine angle of the vectors formed between the point on the trace  $p_i$  to the two terminal points;  $p_s$  and  $p_e$ , given by;

$$\theta_i = \cos^{-1}(\overline{p_s - p_0} \cdot \overline{p_e - p_0} / |\overline{p_s - p_0}| \cdot |\overline{p_e - p_0}|)$$

Taking the second derivative of this angle provides a clear indication of a corner within the trace by forming a spike in the second derivative. We find these spikes in the  $\bar{\theta}$  vector by finding the local maxima by a simple comparison of neighboring values. The trace is split at this spike point  $p_i$ . All the traces are split based on these criteria.

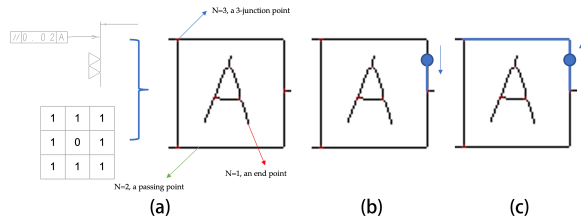


Figure 4: (a) The process to identify the junction points, passing points and end points of a skeletonized drawing. (b) The trajectory tracing process from a passing point to a junction/end point. (c) After (b), another tracing is done to search for the other end of the trajectory.

Subsequently, check for small traces and eliminate them. Traces with  $m_j < 4$  pixels are eliminated to ensure that we don't have an underdefined problem while fitting the cubic bezier curves in the next step. We also merge the terminal points of small traces, so the neighboring traces are now connected. We also merge junction points to ensure the edge-connectivity of the graph. Finally, we fit cubic bezier curves on traces. We use the least square method for fitting the cubic bezier curves as shown in the equation:

$$\bar{\mathbf{p}}^j = [p_0^j, p_1^j, \dots, p_{m_j-1}^j]^T$$

$$B_{i,n_{ord}}^j(t) = \binom{n_{ord}}{i} (t)^i (1-t)^{n_{ord}-i}, i = 0, 1, \dots, n_{ord}, t \in [0, 1]$$

$$\mathbf{B}_{m_j \times (n_{ord}+1)}^j \mathbf{x}_{(n_{ord}+1) \times 2}^j = \bar{\mathbf{p}}_{m_j \times 2}^j$$

Where,  $\bar{\mathbf{p}}^j$  is the ordered list of  $m_j$  points in the  $j^{th}$  trace,  $B_{i,n_{ord}}^j(t)$  is the Bernstein polynomial of order  $n_{ord} = 3$ ,  $\mathbf{B}^j$  is the Bernstein matrix of the cubic bezier curve and  $\mathbf{x}^j$  is the control points for the  $j^{th}$  trace. We set the terminal points as the first and last points of the bezier curve control points. i.e.  $x_0^j = p_s^j$  and  $x_3^j = p_e^j$ .

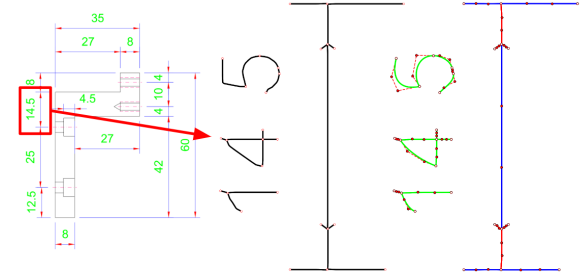


Figure 5: Raster drawing with the highlighted region showing the thinned pixels with junction points and subsequently the cubic bezier curves fitted on the traces with their respective control points.

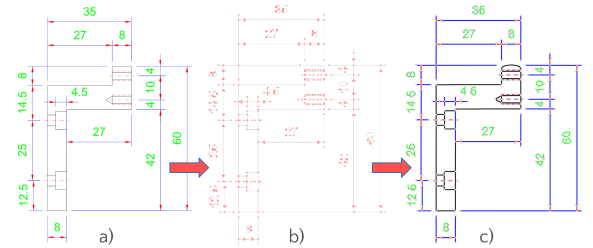


Figure 6: (a) Raster drawing (b) Thinned, smoothed and traced trajectories with junction points marked in red circles (c) Cubic bezier curves fitted on pixel traces.

These steps provide the necessary set of parameterized vectors needed for the construction of a unified graph used in our approach for segmenting the engineering drawing into its various components.

### 3.2. Graph Construction

At the heart of our proposed method, a graph representation for the components is the key to embedding topological features and contextual information among the distant but connected components. In our graph structure, the node vectors are obtained from our vectorization. The graph edges are generated from the connection between these vectors. To form a unified representation, we sample  $n$  evenly spaced points along each vector for featurization. Tab. 1 lists the features

Table 1: Our proposed nodal features.  $n$  is the number of sampled points on each vector.

Feature Type	Parameter	Dimension
Shape	$n$ points sampled along the trace, XY coordinate	$2n$
Length	Length between each pair of consecutive points	$n - 1$
	Total length (of the curve)	1
	first-to-last/total	1
Angle	Cos angle between each pair of consecutive short line segments	$n - 2$
Curvature	Curvature at each sampled point	$n$

computed based on these sampled points. The proposed features encode the shape, length, angle, and curvature information from each vector. Note that the entire drawing is normalized to fit in a unit square before being fed into the featurization process to ensure that all features listed are independent of the input drawing size. In summary, our graph model is defined as:

$$G(N, E), N \in \mathbb{R}^{n_N \times (5n-1)}, E \in \mathbb{Z}^{n_E \times 2}$$

where,  $N$  are the nodal features of a graph with  $n_N$  nodes,  $E$  are the edge indices of a graph with  $n_E$  edges. In this way, the target task of this work is converted to predicting the nodal labels. The label, as well as the component type, is defined as  $Y \in \mathbb{Z}_N^n$ . It is a categorical parameter list indicating the type (contour lines, dimension lines, or texts) of each vector.

To establish the ground truth labels  $Y_{gt}$  when creating a dataset for training, we modify a batch renderer for DXF drawings. The renderer EZDXF [41] is modified to be able to parse the component type information stored in the vector DXF drawing and paints each component type with a unique color (Fig. 7). For each vector in the graph, we sample points and check the corresponding color of each point location in the ground truth image. Finally, the ground truth label for each vector is determined by majority voting of the sampled points. In this work, we conduct two testing conditions in terms of the segmentation labels: 1) text/non-text: The model is designed to distinguish the green components vs the other ones. 2) text/contour/dimension: The model is designed to distinguish the green, the black, and the other components. The labels  $Y_{gt}$  are converted to one-hot encoding accordingly.

### 3.3. Graph Segmentation

Based on the graph representation explained above, our task can be represented as:

$$Y \leftarrow F_\theta(G(N, E))$$

where  $G(N, E)$  is our proposed graph structure,  $F_\theta$  is a data-driven model with trainable parameters  $\theta$ ,  $Y$  is the

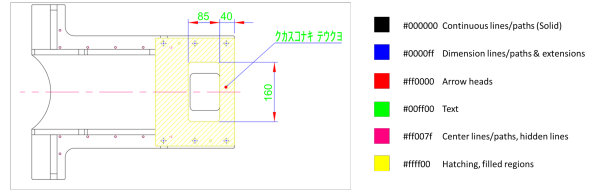


Figure 7: A sample rendering of a DXF drawing used for ground truth label retrieval. Components of each type are painted with a unique color.

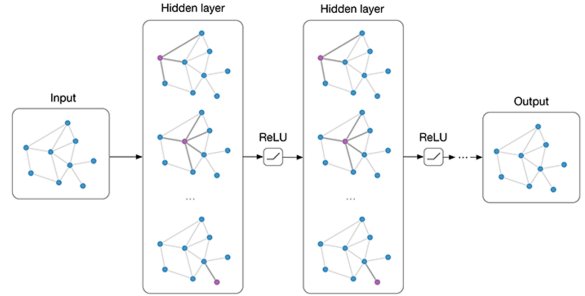


Figure 8: A general structure of GCN.

predicted component type label from the model. During the training of  $F_\theta(\cdot)$ ,  $Y_{gt}$  is utilized for loss calculation. Then, we introduce a model  $F_\theta(\cdot)$ , a loss function  $L$ , and an optimizer to launch the training process.

Graph Convolutional Networks (GCNs) (Fig. 8(a)) are a type of network that works on arbitrarily structured graphs. They have been shown to be effective in various nodal classification tasks including citation and social networks [31, 19]. GraphSAGE model shows superior performance in predicting the nodal class label over the other baseline graph models [19]. Therefore, we build our model based on GraphSAGE. A GCN [31] model and an MLP model are also implemented to serve as baseline models. As a parametric study, we vary the number of convolutional layers in the experiments for the optimized network architecture.

Based on the steps explained above, a graph dataset

is constructed based on 440 real engineering part drawings from the industry. The dataset is split into 80/20 for training and validation. During training, the loss function is chosen as the cross-entropy loss between the predicted nodal class and the ground truth label. Adam [42] optimizer is utilized with a learning rate  $1e-3$ , weight decay  $5e-4$ . All the models are trained with a maximum epoch of 10,000 and batch size of 16. The best model regarding the validation accuracy is saved for inference. In our experiments, each model takes about 20 hours to train on a GeForce RTX 2080 TI Graphics Card.

## 4. Results

This section demonstrates a series of experiments to validate the effectiveness of our graph representation. Additionally, experiment II focuses on optimizing the model architecture with respect to the validation accuracy. Finally, this model setup is extended to a 3-class segmentation problem.

### 4.1. Model Selection

Using our graph representation described in Section 3.2, a classifier is trained to predict the component type of each vector in the drawing. Here, we introduce three data-driven classifiers, including our proposed GraphSAGE model (GS), a vanilla GCN model (GCN) as a graph method baseline, and a Multi-layer Perceptron model (MLP) as a non-graph method baseline in our designed **Experiment I**. To maintain a fair comparison, all three models are designed to have a similar architecture and depth. The details are:

- **GCN** model: 3 vanilla graph convolutional layers+2 linear layers, number of nodes in each hidden layer: [32, 64, 128, 32].  $4 \times \text{ReLU} + 1 \times \text{Softmax}$  as nonlinear activation.
- **GS** model: 3 GraphSAGE convolutional layers+2 linear layers, number of nodes in each hidden layer: [32, 64, 128, 32].  $4 \times \text{ReLU} + 1 \times \text{Softmax}$  as nonlinear activation.
- **MLP** model: 5 linear layers, number of nodes in each hidden layer: [32, 64, 128, 32].  $4 \times \text{ReLU} + 1 \times \text{Softmax}$  as nonlinear activation.

In **Experiment I**, the three models described above are trained with identical training conditions to distinguish the text vs non-text components in our constructed

part drawing dataset. We use  $n = 4$  for the dataset creation in this experiment based on a parametric study detailed in section Appendix A. Fig. 9 illustrates the validation accuracy in the training process. It can be concluded that graph-based models (GS and GCN) yield better ( $> 5\%$ ) results than the non-graph-based model (MLP), which speaks for the necessity of the contextual information embedded in our designed graph structure. Conversely, GS and GCN model share the same pattern in the validation curve in the early phase of the training ( $< 500$  epochs). Then, the GS model rapidly converges at around 1000 epochs to 95%, while the GCN model gradually converges to a lower value at around 3000 epochs. The results confirm the superior capability of our implemented GS model. Next, we want to boost its performance by optimizing the model depth.

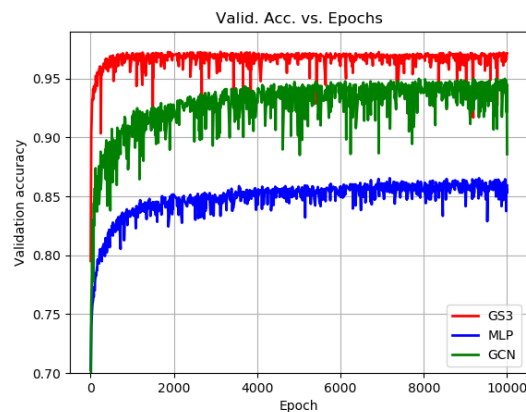


Figure 9: The training curves for GS, GCN and MLP model in **Experiment I**.

### 4.2. Model Depth Study

Through **Experiment I**, the GS model with 3 convolutional layers yields the best performance over the other two models. Therefore, we further design **Experiment II** to study the effect of model depth on the final classification accuracy. Three GS models in this experiment are implemented with 3, 4, and 5 graph convolutional layers. For consistency, all three networks are assembled so that the graph layers expand the dimensions. Then the linear layers squeeze the dimensions to the final desired number of classes. The details are:

- **GS3** model: 3 GraphSAGE convolutional layers+2 linear layers, number of nodes in each hidden layer: [32, 64, 128, 32].  $4 \times \text{ReLU} + 1 \times \text{Softmax}$  as nonlinear activation.

- **GS4** model: 4 GraphSAGE convolutional layers+3 linear layers, number of nodes in each hidden layer: [32, 64, 128, 256, 128, 32]. 6×ReLU +1×Softmax as nonlinear activation.
- **GS5** model: 5 GraphSAGE convolutional layers+4 linear layers, number of nodes in each hidden layer: [32, 64, 128, 256, 512, 256, 128, 32]. 8×ReLU +1×Softmax as nonlinear activation.

We utilize the same setup as Experiment I for training all three models above. Fig. 10 demonstrates the validation curves for these GS models during the training session. We conclude that the performance of the GS model tends to increase for deeper models. However, the improvement gradually levels out when 5 convolutional layers are used. Additionally, Tab. 2 summarizes the confusion matrix for the best model, GS5. Sample prediction results are also demonstrated in Fig. 11. Results show that our GS5 model achieves nearly perfect results in all three test drawings. More statistical comparison results with other baseline models are detailed later in section 4.4. Then, we extend the test condition to multi-class segmentation.

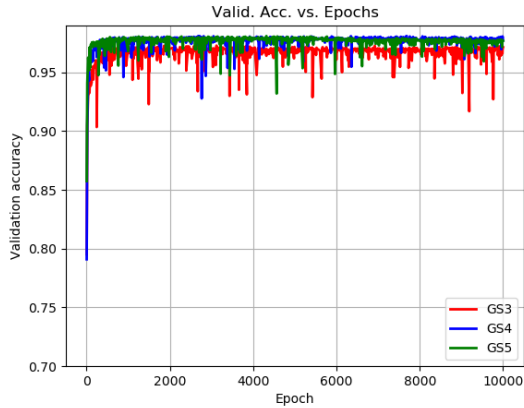


Figure 10: The training curves for GS models of different depths in experiment II.

Table 2: Confusion matrix of our proposed GS5 model in the 2-class segmentation task. From these statistics, the evaluation results can be calculated: **Precision**= 98.38%, **Recall**= 98.57%, **Accuracy**= 98.48%.

GT	Prediction	
	Text	Non-text
Text	21103	304
Non-text	345	13559

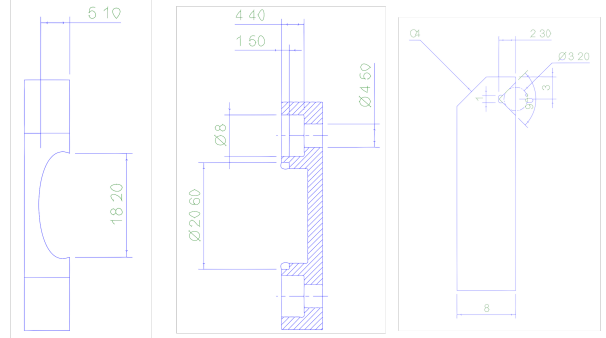


Figure 11: Sample prediction results from GS5 models in experiment II. The colors Green and blue indicate the predicted text components and non-text components respectively.

#### 4.3. Multi-class Segmentation

In previous experiments, the classifier is trained to distinguish between the text and non-text components. This task is relatively simple since text components are usually unique in terms of size and curvature compared to all other straight curves. For practical use, the human inspector needs to comprehend the overall shape of the part through all contour lines, and then gather all manufacturing requirements through dimensions and texts. As such, we construct a dataset with three component types for prediction: Contour, Text, and Dimension, which correspond to black, green, and all other colored lines in Fig. 7. The dataset is utilized in **Experiment III** for training a GS5 model in a 3-class segmentation task for the part drawings.

Table 3: Confusion matrix of our proposed GS5 model in the 3-class segmentation task. Based on the statistics, the performance of the model can be calculated: **Precision**: 83.03%, 95.04%, 90.70%, **Recall**: 83.46%, 96.07%, 89.60%, **Accuracy**: 90.82%.

GT	Prediction		
	Contour	Text	Dimension
Contour	4238	130	710
Text	105	9229	273
Dimension	761	352	9589

The resulting confusion matrix of our proposed model (GS5) is shown in Tab. 3. It can be concluded that the model retains high accuracy on the text components, while the separation between the contour lines and dimension sets is more challenging to learn. Two major types of failure cases are: (1) Isolated small components in the text. For example, misclassification happens on the dashed line, diameter symbol, and through hole symbols in the sample results. A potential cause is that these components are not connected with any other



Table 4: Validation accuracy comparison results in three segmentation tasks.

Validation Accuracy %	PSPNet	DeepLabV3	Sketchgnn	EDGNet (Ours)
Text/Non-text	96.62	96.87	94.76	<b>98.48</b>
Contour/Non-contour	80.54	82.57	88.10	<b>94.57</b>
Text/Contour/Dimension	79.54	81.64	84.37	<b>90.82</b>

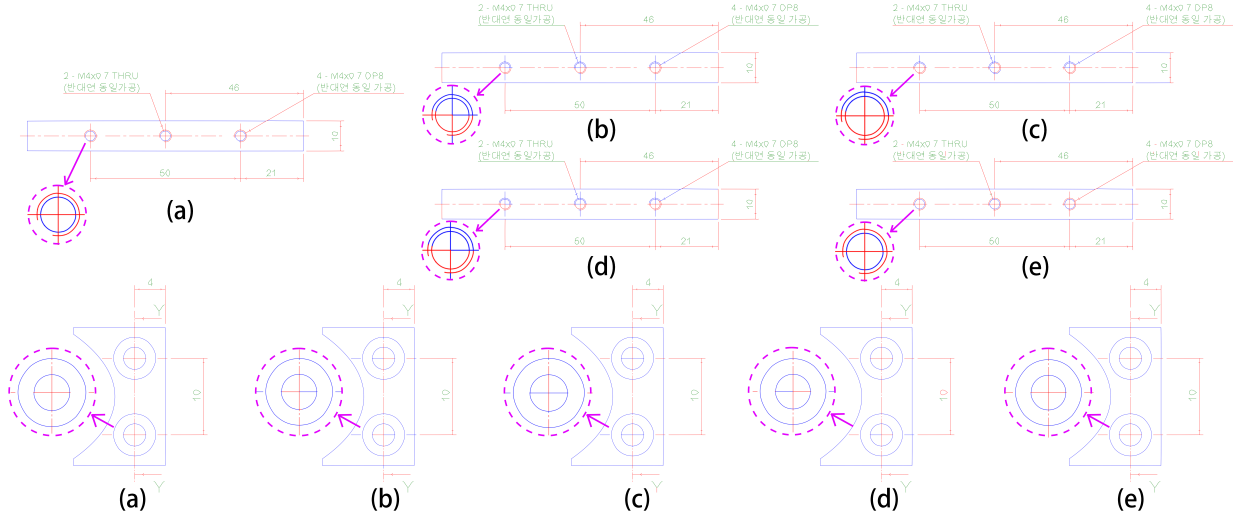


Figure 13: Sample prediction results from three baseline models versus ours. (a) The ground truth. (b) PSPNet results. (c) DeepLabV3 results. (d) Sketchgnn results (e) Ours.

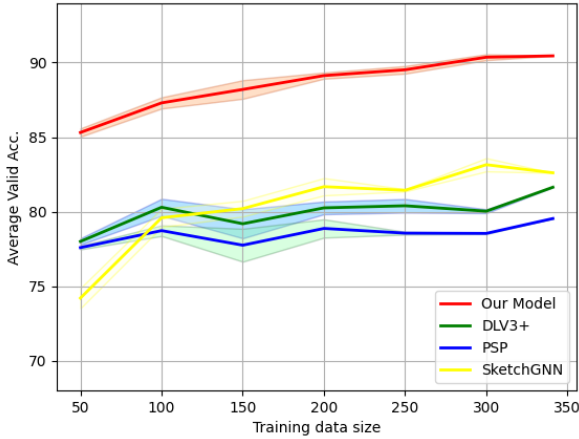


Figure 14: Validation accuracy of the models trained on datasets of various sizes.

angle, the shift and the curvature change between the two connected components can be added to our current graph representation. This information can help the network to understand if two components are truly connected based on semantic meaning or just indepen-

dent of each other with an intersection. With this new graph representation, GraphSAGE model should also be replaced with more advanced graph networks that also take edge attributes as input for analysis, such as Graph Attention Networks [32], Graph Transformers [46], and GINE Convolution [47].

The ultimate goal of our work is to aid a human operator when inspecting drawings for topology and manufacturing information necessary for the later quotation process. The effectiveness of our framework needs to be practically validated by human users. To enable easier access for the system we propose in this work, an interactive user interface should be developed to allow the users to upload their own drawings, launch the vectorization, and get the automatic component type prediction results. Then the user is only responsible for marking the critical information or correcting minor errors in the prediction. Compared to the original inspection and labeling task, the work for the human operator is more efficient and intellectual.

## 6. Conclusions

In this work, we present a novel framework for raster engineering drawing analysis, including a preprocessing method for drawing vectorization, a graph representation embedded with domain knowledge, and a data-driven model to learn and predict the component type of each vector in the drawing. The framework converts the problem from sparse image comprehension into semantic segmentation of the vectorized components from the original drawing, enhancing the efficiency of feature extraction. Results also show that our method yields superior performance in distinguishing the semantic meaning of contour/dimension lines compared to common CNN-based image segmentation methods. A similar framework can be established to other analyses of raster engineering drawings such as manufacturing method classification [48], dimension estimation, and similarity search. The proposed graph representation has the potential to be used extensively in developing a digitized tool for a part quotation.

## Acknowledgement

The authors would like to thank MiSUMi Corporation for their provision of a contemporary engineering problem, guidance on the applicability of developed methods, and financial support. Additionally, the authors appreciate the help from Run Wang, Zhuoran Cheng, Zheren Zhu and Chenlai Wang.

## Appendix A. Parametric Study on $n$

In this study, we vary the number of sampled points on each vector  $n \in \{4, 5, 6, 7, 8, 10, 12\}$  to explore its effect on the final model performance. Like GS3 model detailed in section 4, as  $n$  increases, we enlarge the width of each layer accordingly. The resulting validation accuracies as  $n$  increases are summarized in Fig. A.15. From the figure, it can be concluded that there is no significant changes in validation accuracy as  $n$  varies. A potential cause lies in the fact that the majority of the obtained vectors are straight lines. There is no extra useful information added to the input when more points are sampled in between. The difference when  $n = 4$  and  $n = 12$  can be ignored. But  $n = 12$  requires 3x more parameters to train, which usually leads to much more training time and less stability. As such, we choose  $n = 4$  for all of the experiments for feature exaction.

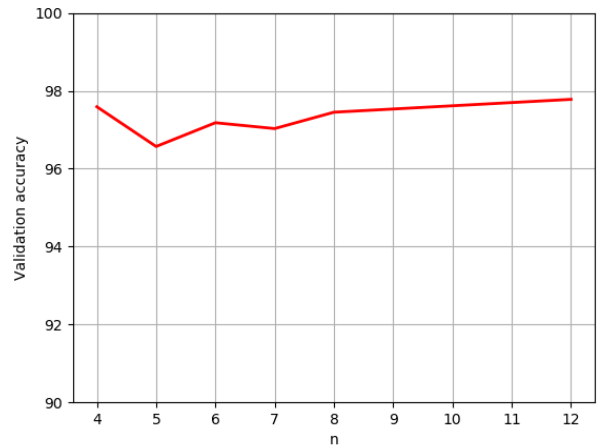


Figure A.15: Validation accuracy of GS model trained on datasets with the number of sampled points  $n$  increases.

## References

- [1] M. J. Fonseca, A. Ferreira, J. A. Jorge, Content-based retrieval of technical drawings, *International Journal of Computer Applications in Technology* 23 (2-4) (2005) 86–100.
- [2] D. R. Kasimov, A. V. Kuchuganov, V. N. Kuchuganov, Individual strategies in the tasks of graphical retrieval of technical drawings, *Journal of Visual Languages & Computing* 28 (2015) 134–146.
- [3] N. Sajadfar, Y. Ma, A hybrid cost estimation framework based on feature-oriented data mining approach, *Advanced Engineering Informatics* 29 (3) (2015) 633–647.
- [4] P. Kulkarni, A. Marsan, D. Dutta, A review of process planning techniques in layered manufacturing, *Rapid prototyping journal*.
- [5] L. Mitsubishi UFJ Research & Consulting Co., A survey on projects and issues in Japan’s manufacturing industry, [https://www.meti.go.jp/medi\\_lib/report/2020FY/000066.pdf](https://www.meti.go.jp/medi_lib/report/2020FY/000066.pdf).
- [6] J. Redmon, S. Divvala, R. Girshick, A. Farhadi, You only look once: Unified, real-time object detection, in: *Proceedings of the IEEE conference on computer vision and pattern recognition*, 2016, pp. 779–788.
- [7] K. He, G. Gkioxari, P. Dollár, R. Girshick, Mask r-cnn, in: *Proceedings of the IEEE international conference on computer vision*, 2017, pp. 2961–2969.
- [8] J. Wang, K. Sun, T. Cheng, B. Jiang, C. Deng, Y. Zhao, D. Liu, Y. Mu, M. Tan, X. Wang, et al., Deep high-resolution representation learning for visual recognition, *IEEE transactions on pattern analysis and machine intelligence* 43 (10) (2020) 3349–3364.
- [9] J. Long, E. Shelhamer, T. Darrell, Fully convolutional networks for semantic segmentation (2015). [arXiv:1411.4038](https://arxiv.org/abs/1411.4038).
- [10] O. Ronneberger, P. Fischer, T. Brox, U-net: Convolutional networks for biomedical image segmentation (2015). [arXiv:1505.04597](https://arxiv.org/abs/1505.04597).
- [11] L.-C. Chen, Y. Zhu, G. Papandreou, F. Schroff, H. Adam, Encoder-decoder with atrous separable convolution for semantic image segmentation, in: *Proceedings of the European conference on computer vision (ECCV)*, 2018, pp. 801–818.
- [12] L. H. Li, M. Yatskar, D. Yin, C.-J. Hsieh, K.-W. Chang, Visualbert: A simple and performant baseline for vision and language, [arXiv preprint arXiv:1908.03557](https://arxiv.org/abs/1908.03557).
- [13] H. Jiang, I. Misra, M. Rohrbach, E. Learned-Miller, X. Chen, In defense of grid features for visual question answering, in: *Proceedings of the IEEE/CVF Conference on Computer Vision and Pattern Recognition*, 2020, pp. 10267–10276.
- [14] W. Wang, H. Bao, L. Dong, F. Wei, Vlmo: Unified vision-language pre-training with mixture-of-modality-experts, [arXiv preprint arXiv:2111.02358](https://arxiv.org/abs/2111.02358).
- [15] I. Bhattacharya, L. Getoor, Collective entity resolution in relational data, *ACM Transactions on Knowledge Discovery from Data (TKDD)* 1 (1) (2007) 5–es.
- [16] P. Sen, G. Namata, M. Bilgic, L. Getoor, B. Galligher, T. Eliassirad, Collective classification in network data, *AI magazine* 29 (3) (2008) 93–93.
- [17] S. Fakhraei, D. Sridhar, J. Pujara, L. Getoor, Adaptive neighborhood graph construction for inference in multi-relational networks, [arXiv preprint arXiv:1607.00474](https://arxiv.org/abs/1607.00474).
- [18] G. Namata, B. London, L. Getoor, B. Huang, U. Edu, Query-driven active surveying for collective classification, in: *10th International Workshop on Mining and Learning with Graphs*, Vol. 8, 2012, p. 1.
- [19] W. Hamilton, Z. Ying, J. Leskovec, Inductive representation learning on large graphs, *Advances in neural information processing systems* 30.
- [20] A. Mednionogov, V. Kyrki, H. Kälviäinen, Content-based matching of line-drawing images using the hough transform, *IJDAR* 3 (2000) 117–124. [doi:10.1007/s100320070001](https://doi.org/10.1007/s100320070001).
- [21] L. Jiao, F. Huang, Z. Teng, An engineering drawings retrieval method based on density feature and improved moment invariants, *Proceedings of the 2009 International Symposium on Information Processing (ISIP’09)*.
- [22] R. Liu, Y. Wang, T. Baba, D. Masumoto, Shape detection from line drawings with local neighborhood structure, *Pattern Recognition* 43 (5) (2010) 1907–1916.
- [23] P. Sousa, M. J. Fonseca, Sketch-based retrieval of drawings using spatial proximity, *Journal of Visual Languages & Computing* 21 (2) (2010) 69–80.
- [24] G. Feng, C. Viard-Gaudin, Z. Sun, On-line hand-drawn electric circuit diagram recognition using 2d dynamic programming, *Pattern Recognition* 42 (12) (2009) 3215–3223.
- [25] B. Huet, N. J. Kern, G. Guarascio, B. Merialdo, Relational skeletons for retrieval in patent drawings, in: *Proceedings 2001 International Conference on Image Processing (Cat. No. 01CH37205)*, Vol. 2, IEEE, 2001, pp. 737–740.
- [26] X. Zhu, *Semi-supervised learning with graphs*, Carnegie Mellon University, 2005.
- [27] Z. Xiaojin, G. Zoubin, Learning from labeled and unlabeled data with label propagation, *Tech. Rep.*, Technical Report CMU-CALD-02–107, Carnegie Mellon University.
- [28] A. Grover, J. Leskovec, node2vec: Scalable feature learning for networks, in: *Proceedings of the 22nd ACM SIGKDD international conference on Knowledge discovery and data mining*, 2016, pp. 855–864.
- [29] Z. Yang, W. Cohen, R. Salakhudinov, Revisiting semi-supervised learning with graph embeddings, in: *International conference on machine learning*, PMLR, 2016, pp. 40–48.
- [30] B. Perozzi, R. Al-Rfou, S. Skiena, Deepwalk: Online learning of social representations, in: *Proceedings of the 20th ACM SIGKDD international conference on Knowledge discovery and data mining*, 2014, pp. 701–710.
- [31] M. Welling, T. N. Kipf, Semi-supervised classification with graph convolutional networks, in: *J. International Conference on Learning Representations (ICLR 2017)*, 2016.
- [32] P. Veličković, G. Cucurull, A. Casanova, A. Romero, P. Lio, Y. Bengio, Graph attention networks, [arXiv preprint arXiv:1710.10903](https://arxiv.org/abs/1710.10903).
- [33] F. Monti, D. Boscaini, J. Masci, E. Rodola, J. Svoboda, M. M. Bronstein, Geometric deep learning on graphs and manifolds using mixture model cnns, in: *Proceedings of the IEEE conference on computer vision and pattern recognition*, 2017, pp. 5115–5124.
- [34] J. Shi, J. Malik, Normalized cuts and image segmentation, *IEEE Transactions on pattern analysis and machine intelligence* 22 (8) (2000) 888–905.
- [35] D. Stutz, A. Hermans, B. Leibe, Superpixels: An evaluation of the state-of-the-art, *Computer Vision and Image Understanding* 166 (2018) 1–27.
- [36] R. Achanta, A. Shaji, K. Smith, A. Lucchi, P. Fua, S. Süsstrunk, Slic superpixels compared to state-of-the-art superpixel methods, *IEEE transactions on pattern analysis and machine intelligence* 34 (11) (2012) 2274–2282.
- [37] K. Simonyan, A. Zisserman, Very deep convolutional networks for large-scale image recognition, [arXiv preprint arXiv:1409.1556](https://arxiv.org/abs/1409.1556).
- [38] T. Y. Zhang, C. Y. Suen, A fast parallel algorithm for thinning digital patterns, *Communications of the ACM* 27 (3) (1984) 236–239.
- [39] T.-C. Lee, R. L. Kashyap, C.-N. Chu, Building skeleton models via 3-d medial surface axis thinning algorithms, *CVGIP: Graph-*

- ical Models and Image Processing 56 (6) (1994) 462–478.
- [40] A. Datta, S. K. Parui, A robust parallel thinning algorithm for binary images, *Pattern recognition* 27 (9) (1994) 1181–1192.
  - [41] Python package index - pypi.  
URL <https://pypi.org/>
  - [42] D. P. Kingma, J. Ba, Adam: A method for stochastic optimization, arXiv preprint arXiv:1412.6980.
  - [43] H. Zhao, J. Shi, X. Qi, X. Wang, J. Jia, Pyramid scene parsing network, in: *Proceedings of the IEEE conference on computer vision and pattern recognition*, 2017, pp. 2881–2890.
  - [44] L.-C. Chen, G. Papandreou, F. Schroff, H. Adam, Rethinking atrous convolution for semantic image segmentation, arXiv preprint arXiv:1706.05587.
  - [45] L. Yang, J. Zhuang, H. Fu, X. Wei, K. Zhou, Y. Zheng, Sketchgnn: Semantic sketch segmentation with graph neural networks, *ACM Transactions on Graphics (TOG)* 40 (3) (2021) 1–13.
  - [46] V. P. Dwivedi, X. Bresson, A generalization of transformer networks to graphs, arXiv preprint arXiv:2012.09699.
  - [47] W. Hu, B. Liu, J. Gomes, M. Zitnik, P. Liang, V. Pande, J. Leskovec, Strategies for pre-training graph neural networks, arXiv preprint arXiv:1905.12265.
  - [48] L. Xie, Y. Lu, T. Furuhashi, S. Yamakawa, W. Zhang, A. Regmi, L. Kara, K. Shimada, Graph neural network-enabled manufacturing method classification from engineering drawings, *Computers in Industry* 142 (2022) 103697.